http://dx.doi.org/10.5012/bkcs.2014.35.7.2057

Thermochemical Sulfate Reduction Simulation Experiments on the Formation and Distribution of Organic Sulfur Compounds in the Tuha Crude Oil

Changtao Yue,[†,*] Shuyuan Li,[†] and He Song[‡]

[†]*State Key Laboratory of Heavy Oil Processing, China University of Petroleum, Beijing 102249, China*
[*]*E-mail: yuect@cup.edu.cn*
[‡]*Research Institute of Petroleum Engineering of CNPC, Tanggu, Tianjin 300451, China*
Received December 4, 2013, Accepted March 17, 2014

Thermochemical sulfate reduction (TSR) was conducted in autoclave on the system of crude oil and $MgSO_4$ at different temperatures. Gas chromatography pulsed flame photometric detector (GC-PFPD) was used to detected the composition of organic sulfur compounds in oil phase products. The results of the analysis indicate that with increased temperature, the contents of organic sulfur compounds with high molecular weight and thermal stability, such as benzothiophenes and dibenzothiophenes, gradually became dominated. In order to gain greater insight into the formation and distribution of organic sulphur compounds from TSR, positive ion electrospray Fourier transform ion cyclotron resonance mass spectrometry (FT-ICR MS) was used in detecting the detailed elemental composition and distribution of them. The mass spectra showed that the mass range of sulfur compounds was 200-550 Da. Four sulfur class species, S_1, N_1S_1, O_1S_1 and O_2S_1, were assigned in the positive-ion spectrum. Among the identified sulfur compounds, the S_1 class species was dominant. The most abundant S_1 class species increase associated with the DBE value and carbon number increasing which also indicates the evolution of organic sulfur compounds in TSR is from the labile series to the stable one. In pure blank pyrolysis experiments with crude oil cracking without TSR, different composition and distribution of organic sulfur compounds in oil phase products were seen from mass spectra in order to evaluate their pyrolysis behaviors without $MgSO_4$. FT-IR and XRD were used in analyzing the products of solid phases. Two distinct crystallographic phases MgO and $MgSO_4$ are found to coexist in the products which demonstrated the transformation of inorganic sulfur compounds into organosulfur compounds exist in TSR.

Key Words : Thermochemical sulfate reduction, Crude oil, Organic sulfur compounds, Magnesium sulfate, Simulation experiment

Introduction

Sulfur-containing compounds in petroleum are problematic in oil recovery process. The decrease in petroleum resources makes high sulfur-containing crude oil an important choice for our present energy demand.[1] Previous work[2] has shown that sulfur compounds in petroleum may be generated by sulfate from sedimentary environment. When crude oil is expelled from a source rock, it may experience significant chemical alteration due to increased exposure to mineral surfaces, aqueous solutions, and thermal energy. Thermochemical sulfate reduction (TSR) is an abiotic alteration process that commonly occurs in hot carbonate petroleum reservoirs encompassing the reduction of sulfate to sulfide coupled with the oxidation of hydrocarbons to carbon dioxide.[3] Over sixty years ago, TSR was identified by controlled oxidation experiments of organic compounds with sulfates.[4] After that, many experiments have been conducted to study TSR processes and to better understand the composition of TSR impacted gas reservoirs.[5-11] In addition, efforts to simulate TSR experimentally have generally focused on the determination of the reaction kinetics and attempts to understand the details of the reaction mechanisms involved.[4,6,12,13] While a simulation on the TSR origin of organic sulfur compounds (OSCs) using crude oil has not yet been reported.

The formation and distribution of organic sulfur compounds are very important for investigating the source of petroleum, the degree of oil-gas maturity, and the correlation of oil-gas sources. Moreover, the content of them always have great influence on the quality of petroleum. Based on the above discussion, the formation and distribution features of organic sulfur compounds in crude oil still need to be proved by simulation experiments. In this paper, a series of hydrous pyrolysis experiments were conducted involving whole crude oil samples from Tuha oil field in Xinjiang Province with

Table 1. The properties of Tuha crude oil sample

Density g/cm^3	API densiy	Saturates %	Aromatics %	Resins %	Asphaltenes %	Sulfur content %
0.8197	40.21	55.0	30.1	7.9	7.0	0.257

Table 2. Calculated contents sulfur compounds in the oil phase products of Tuha at different temperatures from 350 ºC-450 ºC according to the analysis of GC-PFPD

Sulfur compounds	Contents of sulfurs in the oil phase/μg·g^{-1}				
	350 ºC	375 ºC	400 ºC	425 ºC	450 ºC
Hydrogen sulphide	229.4	262.5	393.2	477.3	358.1
Methyl mercaptan	182.2	228.6	235.9	248.2	175.3
Ethyl mercaptan	147.8	256.5	164.1	133.5	144.3
Ethylmethyl sulfide	464.3	558.6	730.0	761.1	632.4
Propyl mercaptan	98.7	131.6	106.5	122.4	112.2
Thiophene	836.5	1091.3	1170.4	1425.1	1335.5
2-Methyl-1-propane thiol	120.8	172.8	239.4	292.0	363.3
Methyl-isopropyl mercaptan	43.5	61.8	77.2	92.7	146.2
Dimethyl mercaptan	28.7	73.5	46.5	64.5	46.3
n-Butanethiol	93.2	108.2	142.1	128.1	109.3
Ethyl-isopropyl mercaptan	129.1	178.0	156.2	91.5	107.2
Isoamyl mercaptan	52.8	103.2	171.3	132.8	180.4
2-Methylthiophene	752.6	689.3	1029.3	1250.7	912.6
3-Methylthiophene	257.3	289.1	310.6	319.8	489.1
C_2-Thiophene	224.6	283.4	527.1	573.7	982.7
Dipropyl mercaptan	125.5	175.4	310.6	351.3	267.9
C_7-Mercaptan	90.4	113.5	391.2	501.8	325.5
C_3-Thiophene	288	236.5	437.1	516.4	339.5
C_4-Thiophene	123.7	165	252.7	314	169.9
Benzothiophene	516.7	725.2	863.2	957.2	1122.5
C_1-Benzothiophene	276.4	351.8	457.6	516.8	572.7
C_2-Benzothiophene	473.6	607.2	543.2	450.6	351.3
C_3-Benzothiophene	342.4	473.5	508.7	628.2	596.7
Dibenzothiophene	353.2	412.8	622.8	693.7	781.0
C_1-Dibenzothiophene	271.6	352.2	447.9	518.7	557.6
C_2-Dibenzothiophene	251.3	272.8	313.5	347.5	396.0
C_3-Dibenzothiophene	108.7	89.6	162.4	181.4	280.5

and without the presence of $MgSO_4$. In previous works, $MgSO_4$ was reported to be an effective oxidant of hydrocarbons without the addition of hydrogen sulfide, which has been used as an initiator in other experiments.[13,14] In order to gain great insight into the formation and distribution of these organic sulphur compounds from TSR, detailed analyses were performed on the generated oil and residual solids in which some new data were detected by GC-PFPD, FT-ICR MS, FT-IR and XRD.

Experimental

Materials. The crude oil sample is from Tuha oilfield in Xinjiang Province of China. The properties of crude oil are shown in Table 1.

Reaction Conditions. All thermal simulation experiments were carried out at different temperatures. The thermal simulation experiment devices consist of a 200 mL stainless-steel autoclave (100 mm × 50 mm), gas circuit and sampling system. The sample basket is a quartz cylinder (80 mm × 10 mm) with a bottom to hold $MgSO_4$ powder and its other side is left open. The cylinder is placed on the bottom of the reactor. Each time, the cylinder with 20 mL of crude oil is put into the reactor, and then 10.0 g of $MgSO_4$ and 10 mL of distilled water is fed into the reactor before vacuumed. The reaction equation is following:

$$MgSO_4 + C_nH_{2n+2} \rightarrow MgCO_3 + H_2S + S + CO_2 + H_2O$$

The reaction temperatures are 350 °C, 375 °C, 400 °C, 425 °C and 450 °C. Since it is hard to detect any reaction product under temperature lower than 250 °C, so the reactor was first heated to 250 °C directly and then programmed to the final temperatures, and the heating times are 40 h, 35 h, 30 h, 25 h and 20 h, respectively. The autoclave was cooled in the air to room temperature when the desired reaction temperature was attained, and then gaseous product is collected by air pocket (volume 2 L). After the sample basket with solid products is taken out from the autoclave, the mixture of oil and water was drawn from the reactor with a pipette and separated with a micro extraction funnel. The autoclave wall is then rinsed using 10mL distilled water by 3 times. The quartz cylinder with solid products, the separated water, and the rinse solution were all put together into a ceramic crucible. The crucible was kept at 120 °C for 2 h in an oven to remove water, and then calcinated at 550 °C for 2 h in a muffle oven.

Analysis Methods. Gas chromatographic-pulsed flame photometric detective analysis was carried out on an Agilent 7683GC directly coupled to an O.I. Analytical Model 5380 PFPD detector. The separation column was PONA column (50 m × 0.2 mm × 0.5 μm), the injection volume was 1.0 μL, and the split ratio was 30. The entrance temperature was 250 °C with a constant pressure (96.5 kPa) model. The original column temperature was 35 °C and was raised to 100 ºC at a heating rate of 1.5 °C/min, then reached 250 °C at a heating rate of 10 °C/min and the resident time was 15min. Nitrogen was employed as a carrier.

Positive ion ESI FT-ICR MS is now recognized as a powerful analytic technique for resolving and identifying basic heteroatom compounds found in crude oils.[15-19] The samples were analyzed using a Bruker apex-ultra FT-ICR MS equipped with a 9.4T actively shielded superconducting magnet is used to analyze the samples. The operating conditions for positive ion formation were −3.0 kV emitter voltage, −3.5 kV capillary entrance voltage, and 320 V capillary column end voltage. Ions accumulated for 0.01s in a hexapole with 2.4VDC voltage and 300 Vpp RF amplitude. The quadrupole (Q1) was optimized to obtain a broad range for ion transfers. An argon-filled hexapole collision cell was operated at 5 MHz and 400 Vpp RF amplitude, in which ions accumulated for 0.3s. The extraction period for ions from the hexapole to the ICR cell was set to 1.3 ms. The RF excitation was attenuated at 11.75dB, and used to excite ions over the range of *m/z* 200-900. A square sine bell multiplication apodization was carried out, followed by a single zero-fill before fast Fourier transform and magnitude calculation.

FT-IR Analysis. All spectral peaks were recorded from 4000 cm^{-1} to 400 cm^{-1} using the Nicolet FT-IR spectrometer. Each spectrum gave the average value of 32 times scanning with a resolution of 4 cm^{-1}.

XRD Analysis. The products were mechanically crushed and ground as fine as < 75 μm. X-ray diffraction (XRD) data were collected at room temperature from a SHIMADZU X-ray diffractometer under a voltage of 40 kV, a current of 30 mA and a scanning speed of 2 o·min^{-1} with graphite monochromated CuKα radiation. The analytical parameters were divergence slit (DS) = 1°, scattering slit (SS) = 1°, and receiving slit (RS) = 0.3 mm.

Results and Discussion

GC-PFPD Analysis of Oil Phase. According to the results of GC-PFPD Analysis, the calculated contents of organic sulfur compounds at different temperatures are listed in Table 2. The calculated contents of mercaptans, thioethers, thiophenes (TS), benzothiophene (BTS) and dibenzothiophene (DBTS) are respectively exhibited in Figures 1-3.

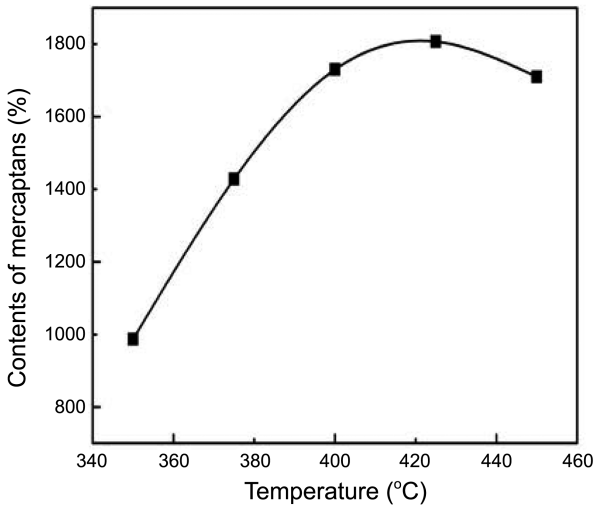

Figure 1. Mercaptans contents of Tuha oil phase products from TSR detected by GC-PFPD at different temperatures from 350 °C to 450 °C.

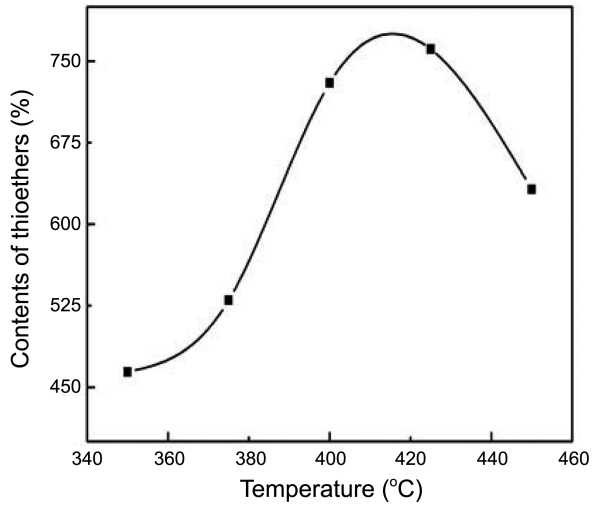

Figure 2. Thioethers contents of Tuha oil phase products from TSR detected by GC-PFPD at different temperatures from 350 °C to 450 °C.

The relationship between the contents of mercaptans and temperature is shown in Figure 1. The variation of the mercaptans contents at the temperature range 350 °C-425 °C is obviously growing, but there is a moderate decline at the temperature range of 425 °C-450 °C, so there is no evident correlation between the content of mercaptans and the temperature. As seen in Figure 2, the content of thioethers has the similar trend to that of mercaptans. This can be attributed to the low thermal stability of mercaptans and thioethers. The contents of mercaptans and thioethers in oil phase products is controlled simultaneously by the generation rate and the thermal decomposition rate that depend on the reaction temperatures. At 350 °C-425 °C, the generation rate of them is superior to the pyrolysis rate leading to the contents of them increase with temperature. But with further temperature increasing, the pyrolysis rate is dominate which makes the contents of them decrease at 425 °C-450 °C coupled with cracking into alkene and hydrogen sulfide. Figure 3 shows the contents of TS, BTS and DBTS at different temperatures. The result shows that the calculated contents of TS are the most dominated in all of the organic sulfur compounds in oil phase products. However, with further increase of the reaction temperature, the conversion of TS into stable organic sulfur compounds like BTS and DBTS due to the poorer thermal stability of TS makes the increase in the contents of BTS and DBTS coinciding with decrease of the TS contents. All these suggest that the conversion of inorganic sulfur to organic sulfur in the whole TSR process, especially to thiophenes, increases with the reaction temperature. In conclusion, the variations of the organic sulfur compouds contents indicates that under the experimental conditions, the TSR produces thermal stable organic sulfur compounds as the final products in oil phase products.

Positive-Ion ESI FT-ICR MS Analysis. Figure 4 shows

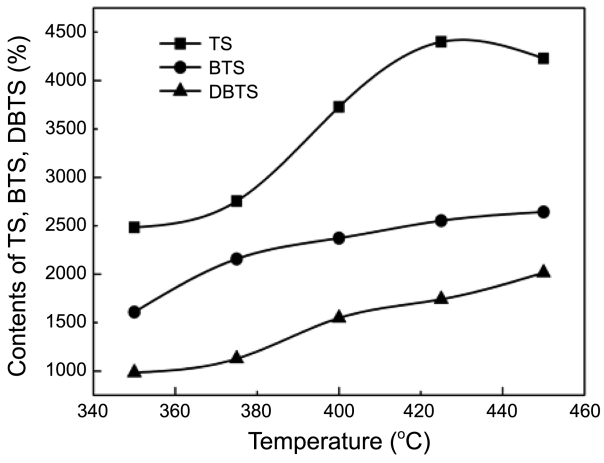

Figure 3. Ts, BTs, DBTs contents of Tuha oil phase products from TSR detected by GC-PFPD at different temperatures at 350 °C-450 °C.

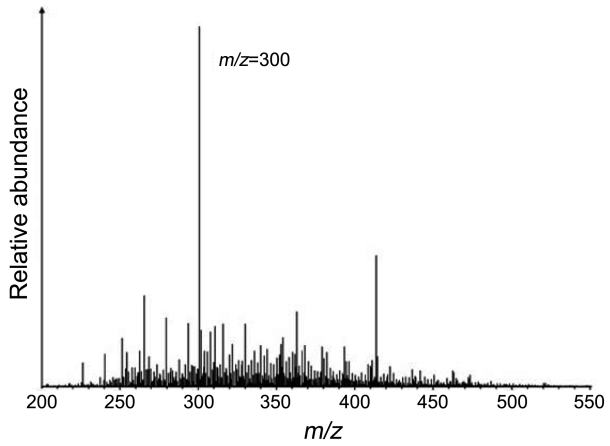

Figure 4. Broad band positive-ion FT-ICR mass spectra of methylated oil phases from TSR simulation at 450 °C The figure shows the dominated mass scale is at m/z = 300.

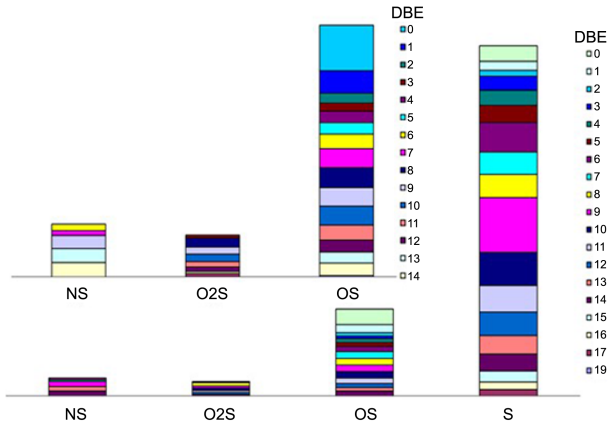

Figure 5. Heteroatom class (number of heteroatoms) and type (DBE) distribution derived from positive-ion ESI FT-ICR mass spectrum of methylated oil phases from TSR simulation at 450 °C.

the positive-ion ESI FT-ICR MS broadband (200Da-550Da) spectrums of methylsulfonium salts derived from TSR under temperature of 450 ºC. The most abundant peaks of TSR sample was at m/z = 300. All of the spectrums were obtained under the resolving power of 554000 (m/Δm50%, at m/z = 339). Elemental compositions of these compounds can be identified by accurate mass analysis.[19-21] The various sulfur compounds identified included S_1, N_1S_1, O_1S_1, and O_2S_1 class species. The relative abundances of heteroatom class species are shown in Figure 5, $S_1 > O_1S_1 > N_1S_1 > O_2S_1$, and the S_1 class sulfur compounds are the dominant species, other classes exhibit low abundances. To examine the molecular composition of various class species, iso-abundance dot-size coded plots are constructed by correlating DBE and carbon number distribution of species.

DBE *versus* Carbon Number for S_1 Class Species. Figure 6 shows the plots of DBE *versus* carbon number for S_1 class species. The high relative abundance S_1 class species has a DBE value of 6-12 and carbon number of 16-26. The minimum DBE value of S_1 class species is 0, because aliphatic hydrocarbons with low isomerization decompose at high temperatures result from pyrolysis. This suggested the presence of sulfides. The S_1 species with DBE of 1 and 2

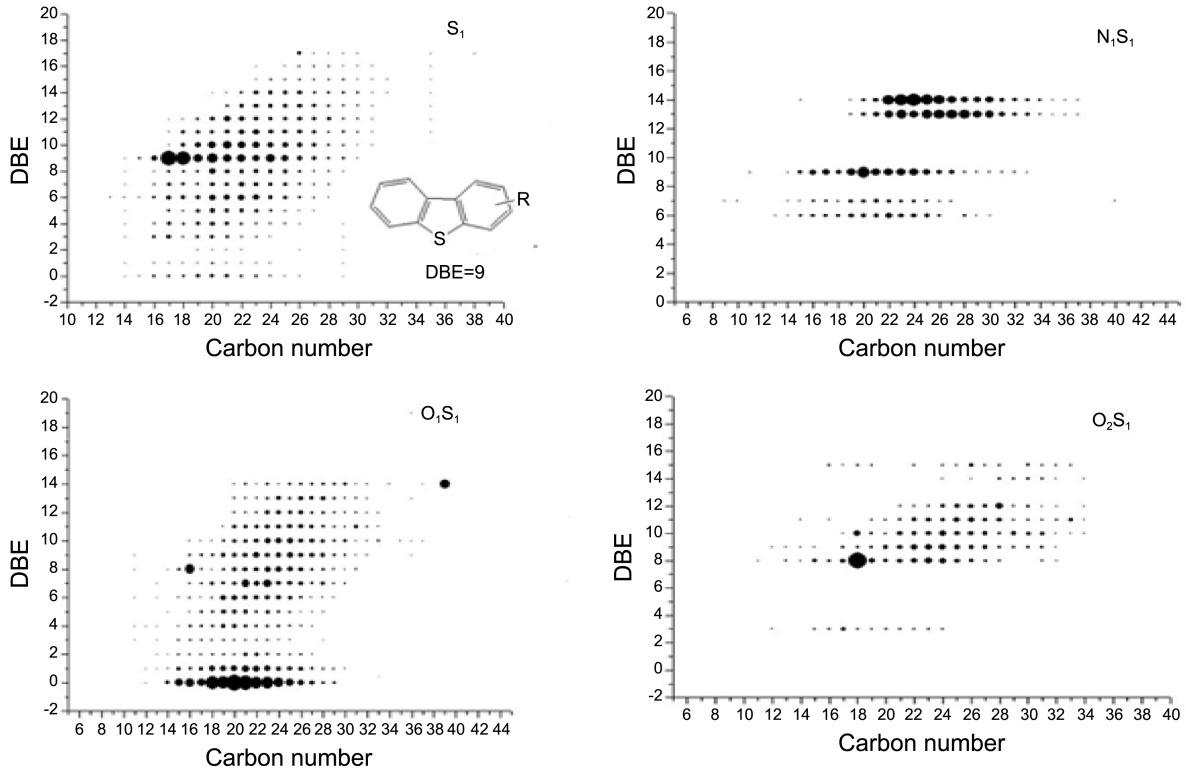

Figure 6. Plots of double bond equivalence (DBE) as a function of carbon number for the different heteroatomic compounds derived from positive-ion ESI FT-ICR mass spectrum of the methylsulfonium salts derived from TSR oil phase product after 450 ºC.

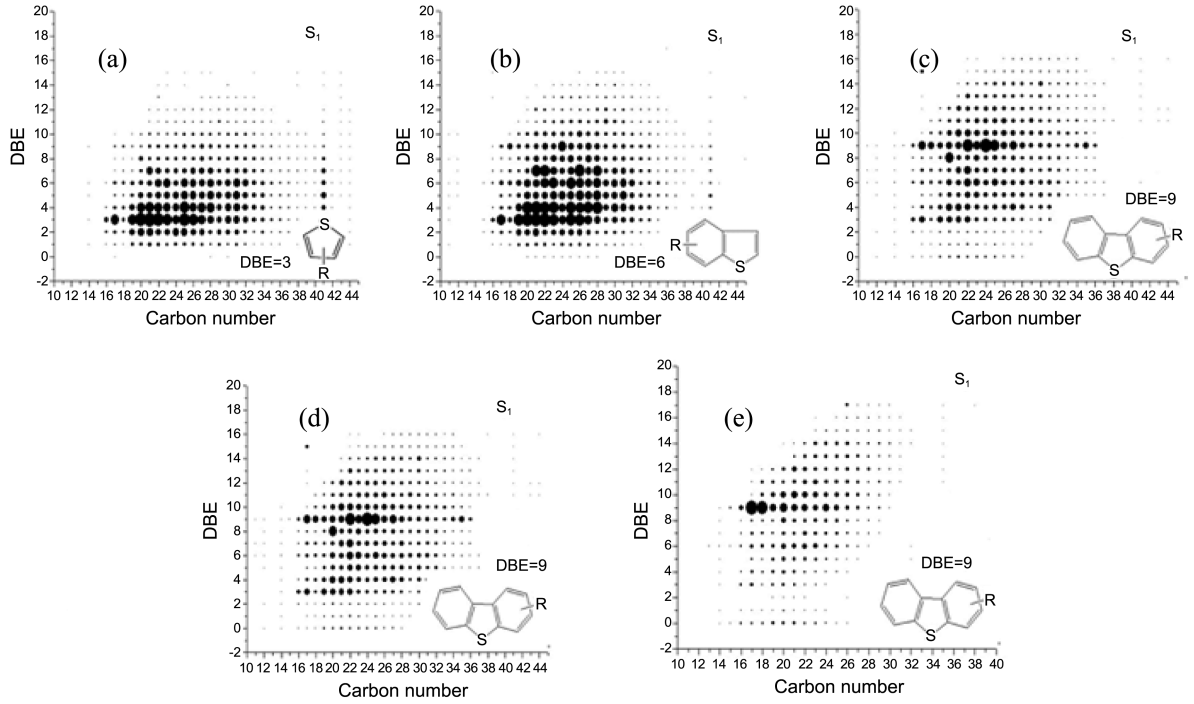

Figure 7. Plots of double bond equivalence (DBE) as a function of carbon number for The largest dots denote the most abundant S1class species derived from positive-ion ESI FT-ICR mass spectrum of the methylsulfonium salts of TSR oil phase product at different temperatures from 350 °C-450 °C. (a) 350 °C (b) 375 °C (c) 400 °C (d) 425 °C (e) 450 °C.

correspond with the one and two cyclic-rings sulfides respectively. Species with DBE of 3 correspond with thiophenes. So the predominant species with DBE value of 6 were benzothiophenes and those with DBE value of 9 were dibenzothiophenes.[22]

DBE *versus* Carbon Number for N_1S_1 Class Species. The N_1S_1 class species in Figure 6 are different from other heteroatom compounds. The existence of nitrogen atom makes it easily detected by positive-ion ESI before methylation. However, the relative contents of the N_1S_1 class species are hardly represented through mass spectrogram before methylation, which suggests that there is an evident difference in the ionicity for the N_1S_1 class species by ESI. After methylation, the sulfonium salts become the controlling factor. Compared to sulfonium salts, the nitrogen ion has relative low iconicity, so the ions of the N_1S_1 class species are derived from sulfonium salts. For the methylsulfonium salts in the Tuha sample, the most abundant N_1S_1 class species has a wide distribution with DBE values of 6, 7, 9, 14 and 15 over the carbon number range of 20-30.

DBE *versus* Carbon Number for O_1S_1 Class Species. The plots of DBE *versus* carbon number for members of the O_1S_1 class species is shown in Figure 6. It is shown that the O_1S_1 class species has a relative discrete distribution with DBE values of 0-19. The DBE value of 0 is dominate which suggests the heteroatom compounds are likely sulfides with a hydroxyl. Species with DBE value of 1 are likely cyclic-ring sulfides with a hydroxyl. Compared with DBE value of 11, the O_1S_1 class species with DBE 8 are likely benzofuranthiophenes and DBE value of 11 is dibenzofuranthiophenes.

DBE *versus* Carbon Number for O_2S_1 Class Species. The O_2S_1 class species in Figure 6 are mainly naphthenic acid with a hybridized sulfur atom, according to the analysis of positive-ion ESI FT-ICR MS which detected the structure of O_2 class species is naphthenic acid. The O_2S_1 class species with DBE value of 8 are the most dominated, likely benzothiophenes with a naphthenic acid.

As Figure 7 shown, the general trends of the DBE of the S_1 class species shift to higher values as the reaction temperature increase. The most abundant S_1 class species with DBE values of 2, 3 are likely one and two cyclic-rings sulfides and 4 DBE is likely thiophenes at the temperature range from 350 °C to 375 °C. When the temperature up to 400 °C, the DBE values of 3-10 are dominant corresponding with not only cyclicsulfides and thiophenes but also benzothiophenes and dibenzothiophenes. However, from 425 °C to 450 °C, the S_1 class species with 9 DBE are abundant, which suggests that dibenzothiophenes gradually account for the major part in TSR oil phase products.

Blank Pyrolysis Experiments with Crude Oil. For comparison purposes, thermal cracking experiments on the Tuha crude oils without the presence of $MgSO_4$ were conducted under the same experimental conditions. The results of positive-ion FT-ICR mass spectra from the thermal cracking of the crude oils were detected to explain the impact of TSR on the formation and distribution of sulfur compounds.

Figure 8 shows the positive ESI FT-ICR MS broadband (250-550Da) spectrums of blank pyrolysis experiment sample at temperature of 450 °C. The abundant peaks with even masses in the 250-500 mDa molecular weight range indicated that the molecular weight of the dominant compounds is around 350 mDa. Four sulfur class species S_1, N_1S_1, O_1S_1,

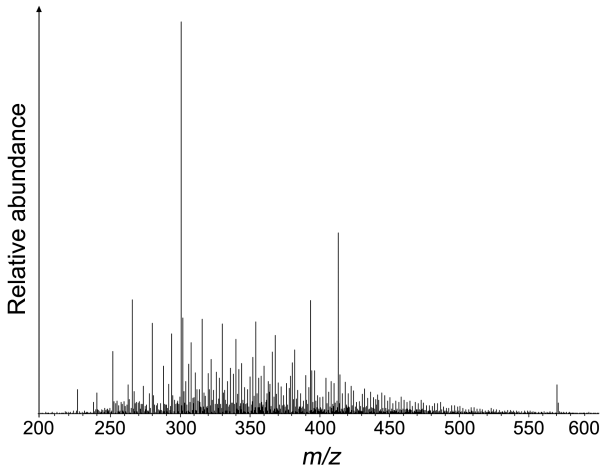

Figure 8. Broad band positive-ion FT-ICR mass spectra of methylated oil phases from blank pyrolysis experiment at 450 °C. The figure shows the dominated mass scale is at m/z = 300.

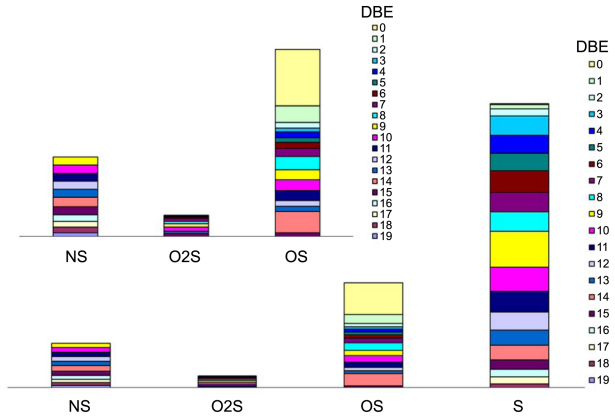

Figure 9. Heteroatom class (number of heteroatoms) and type (DBE) distribution derived from positive-ion ESI FT-ICR mass spectrum of methylated oil phases from blank pyrolysis experiment at 450 °C.

O_2S_1 were assigned in the positive-ion spectrum.

The relative abundances of positive ion heteroatom class species for four sulfur class species are shown in Figure 9. Among the identified sulfur compounds, the S_1 class species was dominant.

Figure 10 shows the plots of DBE *versus* carbon number for the S_1, N_1S_1, O_1S_1 and O_2S_1 class species of pure pyrolysis experiments from the ESI FT-ICR mass spectra. The S1 species has a DBE value of 1-19 and carbon number of 10-55. Apparently, the isoabundance maps of S1class species in blank experiments are different from that of TSR, with wider range of DBE value and carbon number values than those of TSR, indicating that there is only a low molecular condensation in large carbon number molecules rather than the trend of transformation from thiophenes to benzothiophenes.

In comparison to the S_1 class species, the DBE and carbon number distribution of N_1S_1, O_1S_1, O_2S_1 class species were more discrete, irregularly. This indicates that most sulfur compounds from pure pyrolysis experiments only had various degrees of condensation.

FT-IR and XRD Analysis of Solid Products. Some black

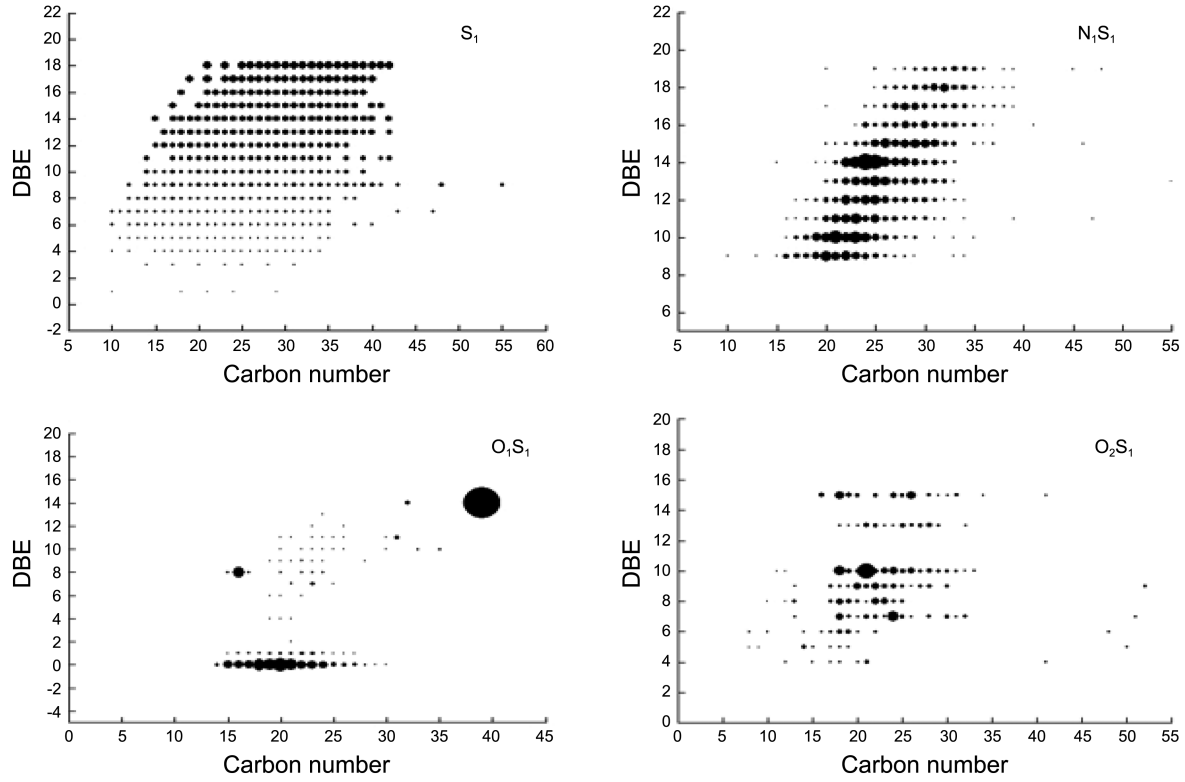

Figure 10. Plots of double bond equivalence (DBE) as a function of carbon number for the different heteroatomic compounds derived from positive-ion ESI FT-ICR mass spectrum of the methylsulfonium salts derived from blank experiments oil phase product after 450 °C.

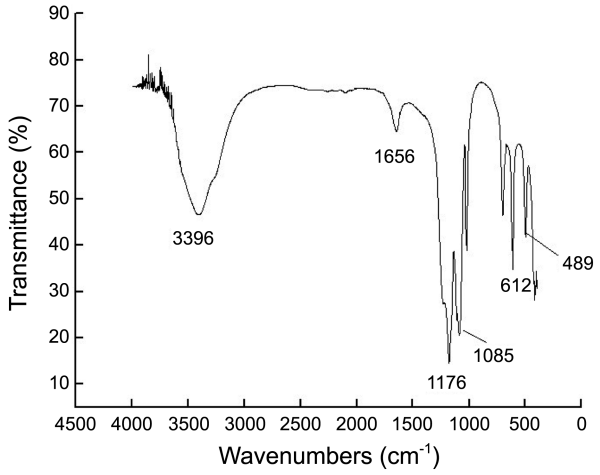

Figure 11. FT-IR spectrum of the solid products after calcination at 450 °C.

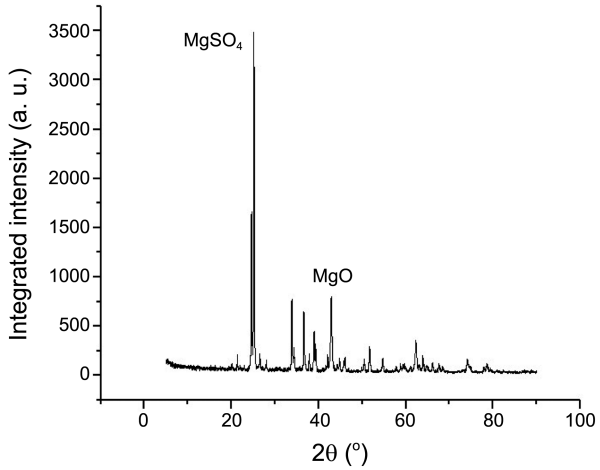

Figure 12. XRD spectrum of the solid products after calcination at 450 °C.

material was observed as the solid product for TSR. After calcination at 550 °C, the black material turns white. Therefore, the black deposit is probably coke. Figure 11 shows the FT-IR spectrums of solid products at the temperature of 450 °C. It is shown that the peaks at 3423 cm^{-1} and 1638 cm^{-1} are the vibrational band of water. This suggests the presence of crystal water in solid. The peak at 1166 cm^{-1} is the vibrational band of sulfate radical. Especially, the appearance of peak at 430 cm^{-1} can be explained by the formation of MgO.[23]

X-ray powder diffraction patterns of solid reaction products at 450 °C are shown in Figure 12. Two distinct crystallographic phases MgO and $MgSO_4$ are found to coexist in the products. It should be noted that the decomposition of magnesium sulphate only take place at temperatures over 1124 °C, but the simulation temperatures are far lower than the decomposition temperature of magnesium sulphate. Therefore, MgO produced should be attributed to the reduction of $MgSO_4$ by hydrocarbons. Because the molecular weight of $MgSO_4$ is bigger than that of MgO, so the weight of solid products after calcinations becomes lighter than the initial weight of solid reactant.

Conclusion

Distribution and formation of organic sulfur compounds in oil phase products and analysis on the residual solids from a series of crude oil pyrolysis experiments in the presence of $MgSO_4$ were carried out.

(1) GC-PFPD is used to investigate the compositions of different organic sulfur compounds in oil phase products. GC-PDPF detected that low thermal stability lead to variations in the content of mercaptans and thioethers coupled with cracking into alkene and hydrogen sulfide with increasing temperature. On the contrary, excellent thermal stability enable the contents of TS, BTS, DBTS increase with temperature.

(2) FT-ICR MS is used to investigate the molecular structure and mass distribution of the organic sulfur compounds. Under our experimental conditions, four class species S1, N1S1, O1S1, O2S1, were assigned in the positive-ion spectrum. The S1 class sulfur compounds are the most dominant species in the oil phase products.

(3) Experiments without $MgSO_4$ indicate that there is a transformation from laible sulfur compounds to stable sulfur compounds exist in the TSR. A quantitative evaluation of the magnitude of this effect will require further work.

(4) FT-IR and XRD analyses suggest that the transformation of inorganic sulfur from sulfate into organic sulfur compounds exist in the TSR system of crude oil and magnesium sulfate.

Acknowledgments. This work was supported by Open Project of State Key Laboratory of Petroleum Resources and Prospecting, China (201107).

References

1. Liang, C. L. *High Sulfur Crude Oil Processing*; Beijing: China Petrochemical Press: 2001.
2. Orr, W. L. *Aapg. Bull.* **1974**, *58*, 2295-2318.
3. Seewald, J. S. *Nature* **2003**, *426*(6964), 327-333.
4. Toland, W. G. *J. Am. Chem. Soc.* **1960**, *82*, 1911-1916.
5. Kiyosu, Y.; Krouse, H. R. *Geochem. J.* **1993**, *27*, 49-57.
6. Cross, M. M.; Manning, D. A. C.; Bottrell, S. H.; Worden, R. H. *Org. Geochem.* **2004**, *35*, 393-404.
7. Yue, C. T.; Li, S. Y.; Ding, K. L.; Zhong, N. N. *Sci. China Ser. D* **2005**, *48*, 1197-1202.
8. Ding, K. L.; Li, S. Y.; Yue, C. T.; Zhong, N. N. *J. Fuel Chem. Technol.* **2007**, *35*, 401-406.
9. Zhang, T. W.; Ellis, G. S.; Wang, K.-S.; Walters, C. C.; Kelemen, S. R.; Gillaizeau, B.; Tang, Y. *Org. Geochem.* **2007**, *38*, 897-910.
10. Chen, T. S.; He, Q.; Lu, H.; Peng, P.; Liu, J. Z. *Sci. China Ser. D* **2009**, *52*, 1550-1558.
11. Lu, H.; Chen, T. S.; Liu, J. Z.; Peng, P. A.; Lu, Z. H.; Ma, Q. L. *Org. Geochem.* **2010**, *41*, 1189-1197.
12. Kiyosu, Y. *Chem. Geol.* **1980**, *30*, 47-56.
13. Goldhaber, M. B.; Orr, W. L. In: Vairavamurthy, M. A., Schoonen, M. A. A., Eds.; *Geochemical Transformations of Sedimentary Sulfur*; ACS Symposium Series, vol. 612. American Chemical Society, Washington, DC, 1995; pp 412-425.
14. Hoffmann, G. G.; Steinfatt, I. In: *Proceedings of the 205th ACS*

National Meeting Enhanced Oil Recovery Symposium (Denver, 3/28/93–4/2/93) Proceedings 38, 1993; pp 181-184.
15. Klein, G. C.; Rodgers, R. P.; Marshall, A. G. *Fuel* **2006**, *85*(14-15), 2071-2080.
16. Shi, Q.; Xu, C. M.; Zhao, S. Q.; Chung, K. H.; Zhang, Y. H.; Gao, W. *Energy Fuels* **2009**, *24*(1), 563-569.
17. Bae, E.; Na, J. G.; Chung, S. H.; Kim, H. S.; Kim, S. *Energy Fuels* **2010**, *24*(4), 2563-2569.
18. Qian, K.; Rodgers, R. P.; Hendrickson, C. L.; Emmett, M. R. *Energy Fuels* **2001**, *15*(2), 492-498.
19. Müller, H.; Andersson, J. T.; Schrader, W. *Anal. Chem.* **2005**, *77*(8), 2536-2543.
20. Purcell, J. M.; Juyal, P. D.; Kim, G.; Rodgers, R. P.; Hendrickson, C. L.; Marshall, A. G. *Energy Fuels* **2007**, *21*(5), 2869-2874.
21. Panda, S. K.; Schrader, W.; Andersson, J. T. *Anal. Bioanal. Chem.* **2008**, *392*(5), 839-848.
22. Kim, Y.; Kim, S. *J. Am. Soc. Mass Spectrom.* **2010**, *21*(3), 386-392.
23. Peng, W. S.; Liu, G. K. *The Charts of the Infrared Spectra of the Minerals (in Chinese)*; Beijing: Science Press, 1982.